Korean J. of Chem. Eng., **7**(2) (1990) *100-108*

INHIBITION OF BUBBLE COALESCENCE BY THE ELECTROLYTES

Jong Won KIM*, Jae Hwa CHANG and Won Kook LEE**

Department of Chemical Engineering, Korea Advanced Institute of Science and Technology, Seoul 136-791
*Korea Institute of Energy and Resources, Taejeon
(Received 7 September 1989 • accepted 18 January 1990)

Abstract—Coalescence frequency and coalescence time were measured in electrolyte solutions. Marrucci model was acceptable to predict the coalescence time of one pair bubble in the dilute solution of electrolytes. Transition concentration decreased with increase of bubble forming frequency. This tendency was same as the results in low molecular alcohol solution.

For a bubble column study, the effects of electrolyte on the gas holdup and bubble characteristics were investigated. The inhibition effect of bubble coalescence of the K_2SO_4 was slightly higher than that of the KCl at a same ionic strength. In this work, transition concentration was 0.36 kmol/m^3, which is larger than the value predicted in pair bubble study.

INTRODUCTION

The knowledge of the coalescence behavior of bubbles in various liquids and solutions becomes important to improve the performance of bubble columns or distillation towers, and a vast number of papers have been reported in the broad fields [1-6]. In spite of considerable research, however, the mechanism of bubble coalescence is still unclear. Traditionally, bubble coalescence phenomena have been studied on a swarm of bubbles in a gas-liquid contacting equipment [1,2] or on a pair of bubbles [3-6].

Correlations and experimental data for the average holdup in bubble columns are ubiquitous in the literature, however, the large scatter in the reported data does not allow a single correlation. This large scatter is mainly due to the extreme sensitivity of bubble coalescence to the materials in the system and to the trace impurities, which is not well understood [7]. Namely, physical properties such as density, viscosity or surface tension could not explain an observed phenomenon in a bubble column completely, especially, in commercial processes in which trace amounts of surface active impurities are frequently present.

The retardation of bubble coalescence caused by the electrolytes is very interesting, and further information of these phenomena is required to apply to various chemical engineering fields.

**To whom all correspondence should be addressed.

The purpose of this work is to investigate the coalescence behavior of contacting bubble grown on adjacent nozzles in the electrolyte solutions. This technique offers a very simple and reliable solution to the surface contamination problem, since fresh clean surfaces are formed shortly before each coalescence event occurs. The coalescence time was measured by an optical sensing method and compared with some mathematical models. Also, the effects of the electrolytes on bubble properties were investigated in a bubble column. Critical transition concentration, which is important for bubble coalescence phenomena, was determined only in side-by-side growing bubbles, because of its simplicity and reproducibility. Experimentally, the transition concentration is defined as the concentration resulting in 50% coalescence percentage. And coalescence percentage is defined as the percent ratio of the number of coalescing pairs over the total number of pairs contacted. The values of critical transition concentration obtained in this work and in literature were compared to the Marrucci parameter [5].

THEORETICAL BACKGROUND

When two bubbles come into contact, a thin liquid film forms between them, draining until an instability forms. Then coalescence occurs. The bubble coalescence mechanism is considered to be a three step process: (1) the approach of two bubbles to within a dis-

Table 1. Properties of gases and electrolyte solutions

System	$\rho_G \times 10^6$ kg·m^{-3}	$\mu_G \times 10^5$ Pa·s	$\rho_L \times 10^3$ kg·m^{-3}	$\mu_L \times 10^3$ Pa·s	σ mN/m	$D^* \cdot 10^9$ m^{2}s^{-1}
Air-KCl (0.1-0.3 kmol/m^3)	1.21	1.83	1.001-1.014	0.998-1.003	72.3-73.2	1.69
Air-K_2SO_4 (0.02-0.1 kmol/m^3)			1.002-1.01	1.006-1.021	72.8-73.2	1.30

*Calculated from the Nernst equation [10].

tance of 10^{-5}-10^{-6} m, (2) further thinning of the liquid layer between the bubbles to a thickness of about 10^{-8}m, (3) rupture of the thin liquid layer via an instability mechanism. The first step is an extremely rapid thinning of the film down to a quasi-equilibrium thickness at which the surface forces on the film are balanced. The quasi-equilibrium thickness is related to the solute concentration at which the transition from mobile to immobile surfaces occurs, and this critical transition concentration can be evaluated by the Marrucci parameter

$$I_{crit}=CRk_e^2/\sigma \tag{1}$$

Whenever the value of Marrucci parameter, I_{crit} is larger than 1.89, the time needed for coalescence is determined by the further thinning of the quasi-equilibrium film down to the rupture, and is described as coalescence time, t_{CO}. Transition concentration derived from the criteria of Marrucci parameter is represented as:

$$c_t=0.084R_GT_e(\sigma A^2/R)^{1/3}(d\sigma/dc)^{-2} \tag{2}$$

This equation will be used to predict coalescence behavior in salt solutions.

The coalescence time, t_{CO}, required for two gas bubbles to coalescence as they approach each other can be calculated from Marrucci's theory. Marrucci [5] suggested a following equation from the mass balance between the film and the out side liquid at any instant.

$$t_{co}=(X_\mu C_o/4D)^2 f^2 I_{crit} \tag{3}$$

where f is a function of I_{crit}, h_o and h_f as described by Marrucci. The Eq. (3) is based on the assumption that complete equilibrium exists between surface and solute concentrations in the film as the film is being stretched. And Marrucci's model allows for the diffusion of solute into the liquid film from the liquid outside the film as a mechanism for film thinning. But Andrew [8] considered a different situation of film thinning. He considered a model where relatively thick film is being stretched, and calculated the increase in surface tension which arises for a given stretching rate as a result of slow diffusion to the surface. According to Andrew's concept, t_{CO} can be computed by:

$$t_{co}=-\frac{\pi}{2DR_G^2T_e^2}\int_{h_o}^{h_f}\frac{[2c(d\sigma/dc)^2+h\Delta P(d\sigma/dc)]^2}{h^3(\Delta P)^2}dh \tag{4}$$

To adapt Eq. (3) and Eq. (4) for predicting coalescence time, initial film thickness (h_o) and final film thickness (h_f) must be well known. In this work, initial and final film thickness were calculated from the approximate expressions, which were used in previous report [9].

EXPERIMENTAL

Potassium chloride and potassium sulfate are used as the electrolyte, and the physical properties of them are listed in Table 1. Bubble column study was carried out in a plexiglas column of 0.1 m i.d. and 1.6 m high as shown in Fig. 1. Oil free compressor air was sparged into the bed through three 6.3 mm i.d. perforated feed pipes with 23 holes of 1 mm i.d. drilled (opening area 0.92%) horizontally and equally spaced with distance of 10 mm, and gas flow rate was measured with rotameter. Four manometer taps were mounted flush with the wall of the column at 0.3, 0.45, 0.9 and 1.05 m above the distributor. The gas holdup was determined by measuring the static pressure with water manometer at four points in the column (static pressure gradient method). The clear liquid height was kept at about 1.2 m. Air was introduced into the bed with desired superficial velocities which ranged from 0.011 to 0.05 m/s. When a steady state was reached, the pressure profile up to the entire height of the column was measured using the liquid manometers. At the same time bubble properties were measured with the bubble probe. The electrical resistivity probe consisted of two needles which were made of chromel-alumel

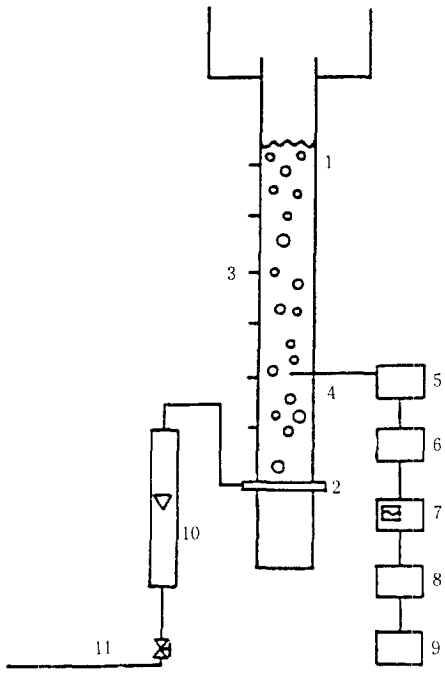

Fig. 1. Experimental set-up for bubble column study.

1. Main column
2. Distributor
3. Pressure tap
4. Probe
5. Probe circuit
6. OP amp.
7. Oscilloscope
8. A/D converter
9. Microprocessor
10. Rotameter
11. Air line

wire with 0.20 mm in diameter and coated with epoxy resin except for the needle tip. The vertical distance between the two tips was maintained 2 mm. The probe was supported by a stainless steel tube which served as an electrode and was placed perpendicularly to the moving direction of the bubbles and at the middle of the column cross section and 0.6 m above the gas distributor. At this location, the effect of sparger design on the bubble size distribution can be neglected and the bubble size distributions have become stationary [11]. This means that a steady state balances of breakup and coalescence is achieved at this height. A dc voltage was applied to the probe and the signals from the probe were amplified and observed by an oscilloscope and stored in a microprocessor through a rapid A/D converter. From these digitized data, the bubble characteristics (vertical bubble length and frequency) were determined. Full details of the data processing are given elsewhere [12].

In pair of bubble, attention was focused to the case of contacting bubbles grown side-by-side. The experimental apparatus used in this work is similar to that of

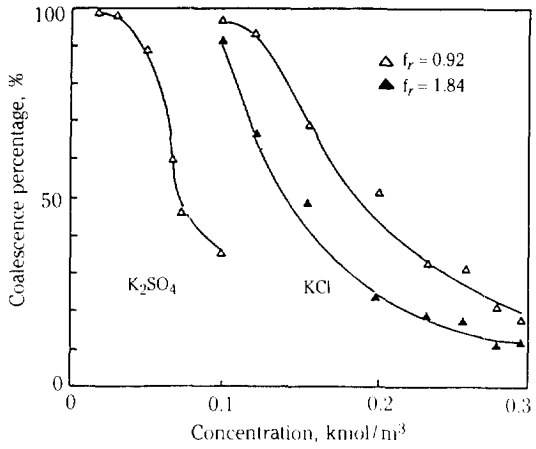

Fig. 2. Bubble coalescence percentage vs. solute concentration.

previous investigators [3,4]. The advantages of the experimental equipment in this work are such that the measuring method of coalescence time is by optical probe, and synchronization of bubbling from two capillaries is by the stepping motor control. Bubbles were formed through two nozzles (No. 14 gauge hypodermic tubing) in a bubble chamber, which was a glass vessel with a thermostatic water jacket and a plate glass window, which permits undistorted observations from outside. The ends of the two nozzles were 0.85 mm apart. Feed gas (nitrogen) was pre-saturated with distilled water and fed to each nozzle through two gas-tight syringes. Gas feed rates were controlled by two variable speed stepping motors which were controlled independently by a microprocessor. The rate of gas injection ranged from 0.007×10^{-6} to 0.076×10^{-5} m^3/s in this work. Bubble coalescence percentage and bubble coalescence time were detected by optical sensing method. The measurement with optical sensing method were described in more detail at the previous paper [9,13]. All experiments were carried out at temperature of $20 \pm 1°C$. The solutions were prepared by using distilled and deionized water whose conductivity was always lower than 10^{-4}S/m.

RESULTS AND DISCUSSION

1. Transition concentration

The coalescence properties are mainly dependent on the added salts. Fig. 2 showed the bubble coalescence percentage vs. solute concentration with solutes or bubble forming frequency. The transition concentration decreased with increase of bubble forming frequency. The transition concentrations at $f_r = 0.92$ and $f_r = 1.84$ were 0.14 and 0.19 kmol/m^3 respec-

Table 2. Ionic strength and transition concentration

Solute	$d\sigma/dc$ ($\mu N \cdot m^2/mol$)	c_t*5, kmol/m^3		ϕ	$c_t(d\sigma/dc)^2$ ($\mu N^2 \cdot m/mol$)	I*6	I_{crit}*7
		Exp.*2	Theoretical*3( )*4				
NaCl	1640	0.175	0.050(0.07)	1.11(1.09)	.471	0.175	6.08
Na_2SO_4	2730	0.061	0.018(0.025)	(1.40)	.455	0.183	5.87
$MgCl_2$	3200	0.055	0.013(0.015)		.563	0.183	7.28
LiCl	1630	0.16	0.051(0.057)	1.06	.425	0.160	5.49
KCl	1440	0.23(0.19)*1	0.065(0.08)	1.12	.477	0.230	6.16
NaBr	1300	0.22	0.080(0.09)		.372	0.22	4.80
$MgSO_4$	2120	0.032	0.030(0.045)		.144	0.15	1.86
K_2SO_4	2580	(0.06)*1	0.020(0.025)		.399	0.18	5.16
$CaCl_2$	3040	0.055	0.014(0.017)		.508	0.165	6.57

*1. This work.
*2. Lessard and Zieminski [14].
*3. From Eq. (2).
*4. Calculated from Oolman and Blanch's model [15].
*5. Referred to the final film thickness at the actual transition concentration.
*6. Ionic strength.
*7. The value at transition concentration.

tively. If a bubble is generated, the concentrations of an electrolyte at the interface and in the bulk liquid are initially equal. However the ions have a tendency to move away from the interface. This results in an enrichment of the liquid phase, accompanied by an increase in the surface tension. If the bubble forming frequency is increased, the surface tension gradient at the bubble surface will be decreased because that the transport of ions in the bulk liquid requires some time. Therefore the coalescence hindering effect of electrolyte will be decreased.

The experimental data of transition concentration in Table 2 were taken from this work and the publications of previous investigators [14,15]. Table 2 showed that observed transition concentration for the various salt solutions is very close to a constant value of the ionic strength, 0.18-0.20. This indicates that the surface activity of the salt solution is primarily dependent on the total concentration of ions in the solution. Also, the actual transition concentrations taken from the literature were compared with those predicted from Eq. (2). The predicted values were lower than the observed value, but this disagreement between theory and experiment is within the precision with which certain of the physical parameters used in the analysis can be estimated. The value of the Hamaker constant and $d\sigma/dc$ are important parameters in the problem that can not be estimated with great accuracy. Also the parameter $c(d\sigma/dc)^2$ at the observed transition concentration was evaluated and was shown in Table 2. The parameter is a measurement of the dynamic surface effect caused by the addition of the solute. Namely, it expresses the degree of easiness for two gas bubble in dilute solution to coalesce. The parameter had the similar value about 4×10^{-4}-5×10^{-4} for each electrolyte. By additionally using the activity coefficient function, ϕ, in the parameter, a better representation of the data might be achieved. At present this is not yet possible because of lack of data on coalescence inhibition for a larger variety of electrolytes and ϕ.

2. Bubble coalescence time

Table 3 showed the bubble coalescence time in electrolyte solutions. K_2SO_4 gave a higher coalescence inhibition effect than KCl did at the same ionic strength.

With disc radius of the order of 0.1 to 1 mm, the distance X_D should be in the range of 1-100 μm or a few percent of the disc radius [6]. The coalescence times at the value of X_D of 1 μm for two electrolytes were shown in Table 3. And this Table showed that the solute having values of I_{crit} in the range 2-10 such as KCl or K_2SO_4 could be adapted to Marrucci's model. This means that diffusion to the surface is fast compared with the time-scale on which the film is stretched. In other words, since the solute diffusion time associated with the electrolyte system is small, complete equilibrium is obtained within the film.

3. Bubble size distribution and gas holdup

It is convenient to define the bubble size distribution as the number fraction of bubbles of a given

Table 3. Comparison of the observed with the predicted values of coalescence times

Solute	c (mol/m^3)	t_{co}(ms) Observed	Andrew model*	Theoretical (Eq. 3)
KCl	100	10	0.653E-3	5.27
	140	15	0.147E-2	20.50
	200	19	0.340E-2	62.00
	230	36	0.465E-2	90.80
	250	51	0.610E-2	124.90
	300	112	0.830E-2	178.10
K_2SO_4	10	14	0.310E-4	0.72
	20	16	0.270E-3	0.92
	30	17	0.800E-3	7.40
	45	20	0.210E-2	38.60
	50	36	0.270E-2	54.60
	70	42	0.580E-2	144.60
	100	110	0.130E-1	355.00

*Calculated from Eq. (4).

size existing in the entire volume of the dispersion. A typical probability density function in this work was shown in Fig. 3, where the distribution exhibits a large deviation from the mean and a high degree of skewness. On the basis of graphical methods, it has been shown that the logarithmic normal distribution most satisfactorily reproduces the original experimental histogram when applied to the distribution of bubble size in a bubble column [16].

The log-normal probability distribution law is given by [17]:

$$P(L_i)=\frac{1}{\sqrt{2\pi}\beta}\exp\left[-\left(\frac{\ln(L_i-\alpha)^2}{2\beta^2}\right)\right] \quad (5)$$

where $\alpha=\ln(L_m)$

$\beta=\ln(\sigma_m)$

and L_i is the vertical bubble length.

Fig. 3 also showed the effect of U_G on the probability density function where the size distribution parameter were taken from the experimental data. The probability density function could be approximately considered a Gaussian curve for a low superficial gas velocity (less than 0.02 m/s). With increasing superficial velocity the peak decrease significantly shifts to higher bubble diameters. This indicates that a redistribution of small bubbles into medium and large bubbles occur. At higher superficial gas velocities large

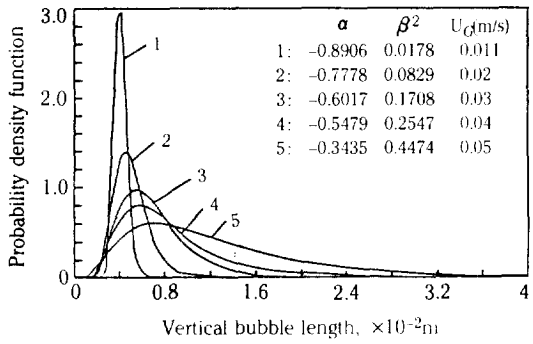

Fig. 3. The effect of superficial gas velocity on the probability density function of vertical bubble length in the bubble column (liqud: tap water).

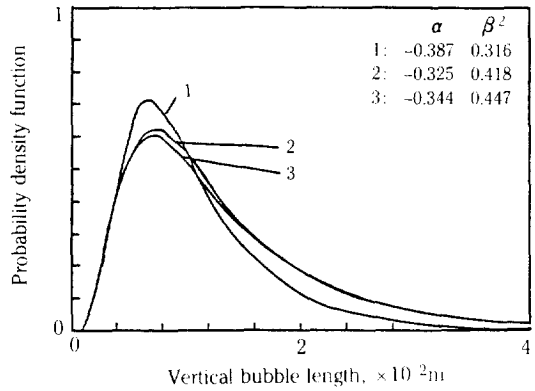

Fig. 4. Probability density function of bubble length in the bubble column (U_G= 0.05 m/s, (1): K_2SO_4 (0.1 kmol/m^3), (2) KCl (0.3 kmol/m^3), (3) tap water).

bubbles arise due to bubble coalescence. The beneficial effect of the gas flow rate upon the coalescence phenomenon could be ascribed to produce a large number of bubbles per unit volume and thus increase the frequency of the collisions in this bubbly flow regime.

The influence of the electrolytes on the bubble size distribution was shown at a constant superficial gas velocity (U_G = 0.05 m/s) and ionic strength (0.3 kmol/m^3) in Fig. 4. Generally at higher concentration, the portion of small vertical bubble length was larger than that at lower concentration. This figure indicated that the inhibition effect of bubble coalescence of the K_2SO_4 was slightly higher than that of the KCl. Fig. 5 showed the probability density distribution curves relative to K_2SO_4 solutions for a superficial gas velocity

Table 4. Coalescence frequency constants

System	C_1	C_2
Tap water	-0.044	21.65
Electrolytes		
KCl 0.1 kmol/m^3	-0.339	28.32
KCl 0.18 kmol/m^3	-0.481	26.30
KCl 0.30 kmol/m^3	-0.457	20.39
K_2SO_4 0.1 kmol/m^3	-0.516	21.52

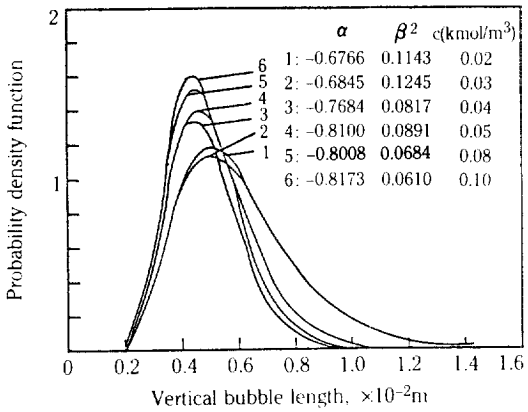

Fig. 5. Variation of probability density function with electrolyte concentration (electrolyte: K_2SO_4, U_G=0.03 m/s).

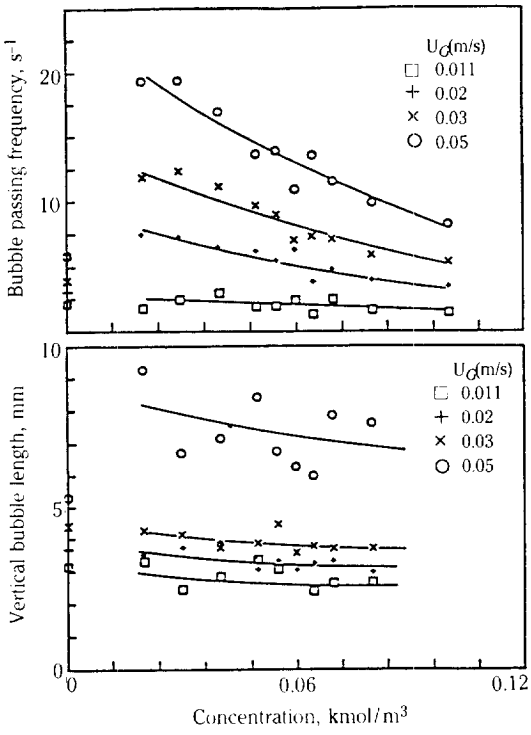

Fig. 6. The effect of the ionic strength on the vertical bubble length and bubble passing frequency. Symbols on the Y-axis mean the values at the orifice plate, which are calculated from the Eq. (6) or Leibson's correlation [20].

of 0.03 m/s. With increasing K_2SO_4 concentration, the curves shifted to the left and became more sharpened. Zieminski and co-workers [14,18] reported that for every electrolyte there is a critical concentration up to which the non-coalescing tendency increases significantly and after which the effect becomes negligible. Marrucci and Nicodemo [19] used a porous plate as a distributor reported the average diameter of the bubbles vs. KCl concentration for a number of superficial gas velocities (0.1×10^{-2}-1.48×10^{-2} m/s). Their results showed that the mean bubble size was constant after reaching an ionic strength (0.23 for KCl) which is same value that observed in the pair bubble study. But when using perforated plates which distribute much larger bubbles, the inhibition of the coalescence processes has a poor effect. Fig. 6 showed the effect of the ionic strength on the vertical bubble length and bubble passing frequency in case of K_2SO_4. The bubble passing frequency is defined as the number of bubbles detected by the lower or upper tip of the bubble probe in a unit sampling time (1 sec). This value is larger than theoretical point bubble frequency, N_p, which is defined as the number of bubbles moved vertically in a unit time.

$$N_p = 1.5U_G/d_B \quad (6)$$

If the bubble moves laterally during measurement, the chord measured by the two tips will be different. Therefore, experimentally, N_p will be measured by rejecting the bubble if this difference is significant. Anyway, bubble passing frequency measured in this work will represent the effect of added salt on bubble characteristics. From the extrapolation according to the slopes, mean bubble size was predicted not to be affected by ionic strength after any ionic strength (0.36) is reached. Therefore, transition concentration can be explained to depend on the gas velocity and sparger design. In addition, the column diameter has some influence if it is small not enough to remove wall effect ($\leq$0.15 m).

The addition of an electrolyte hindered the appearance of large bubbles and results in increased gas holdup values as shown in Fig. 7. It has already been

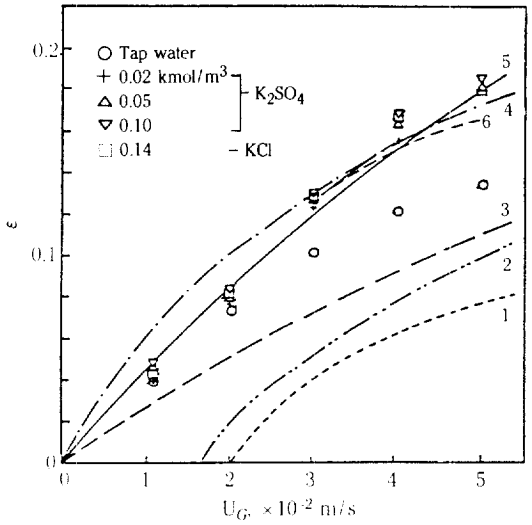

Fig. 7. Gas holdup vs. U_G for; (1) Kim et al. [24]; (2) Akita & Yoshida [20]; (3) Hikita & Kikukawa [25]; (4) Bach & Philhofer [26]; (5) Mersmann [27]; (6) Kelkar et al. [22].

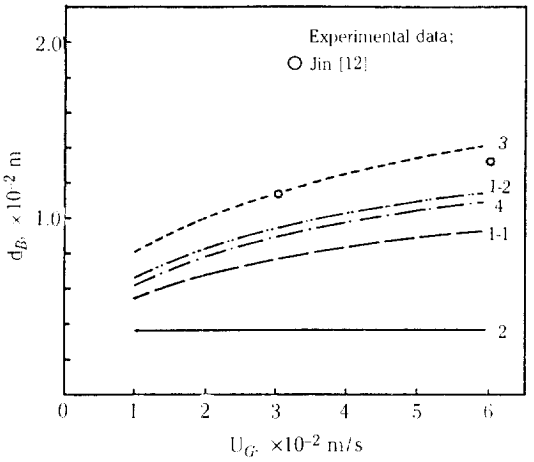

Fig. 8. Initial bubble size in stagnant liquid for; (1) Davidson & Amick[29] (1-1: based on the correlation equation for a single bubble, 1-2: based on the correlation equation for coalescent bubbles); (2) Tate's law; (3) Leibson[30]; (4) Bhavaraju et al. [31].

pointed out in the literature [20-22] that the gas holdup in aqueous electrolyte solutions is slightly larger than that in pure liquids or non-electrolyte solutions. Shah et al. [7] reviewed the voluminous literature on the gas holdup and point out the large discrepancies in these correlations. Fig. 7 showed that the present gas holdup values are higher than those observed by other investigators [20-23]. Probably, this might be due to the use of a different distributor plate. Hikita et al. [21] and Akita and Yoshida [20] both used a single nozzle sparger as a gas distributor, while a perforated plate with holes of 1 mm diameter was used in this work. Freedman and Davidson [23] carried out the holdup experiments with two different distributor plates in the presence of an electrolyte solution and observed that the distributor plate had a significant effect at low gas velocities. A distributor plate having holes of smaller diameter resulted in higher holdup values. An electrolyte solution can maintain this small bubble size by virtue of its non-coalescing tendency. However, Kelkar et al. [22] reported that at higher gas velocities (0.07 m/s or more) this non-coalescing tendency ends, and the bubble size is no longer governed by the distributor plate.

4. Bubble coalescence frequency

Bubble coalescence frequency in the bubble column was analyzed on the base of the concept of Miller [28], which presumed that coalescence occurs as a first rate dependence on mean bubble concentration.

$$N_{BM}=N_{Bo}\exp(-f_c\theta) \tag{7}$$

Two phase holdup time, ϕ, is calculated from two phase volume, V_{TP}, and two phase velocity, U_{TP}.

Bubble concentrations for either mean or initial conditions are obtained from the data about gas holdup, ε, and bubble size. All factors are same as those described by Miller.

Numerous investigators have examined the process of bubble generation, and a number of correlations for predicting the initial bubble size at orifice plate are available in the literature. Fig. 8 showed the comparison of calculated bubble size to the experimental value. The Leibson's correlation [30] was agreed well with the experimental value in this system.

The relation between the vertical bubble length and equivalent diameter can be written as [11]:

$$d_B=2.547L_t. \tag{8}$$

The frequency of bubble coalescence is a function of bulk liquid flow, gas flow and gas holdup in a column. Miller assumed that the coalescence frequencies have the following dependence on two phase velocity:

$$f_c=C_1U_{TP}+C_2U_{TP}^2 \tag{9}$$

and the constants for each system were given in Table 4 and the coalescence frequency vs. two phase velocity curves were shown in Fig. 9.

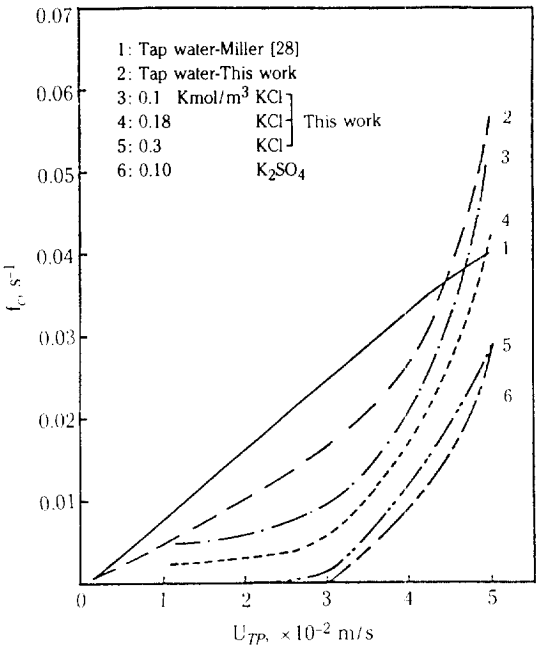

Fig. 9. Coalescence frequency vs. two phase velocity.

Miller [28] found the frequency, f_c, to be of the order of 0.02-0.07 s^{-1} for air-water systems. This work showed that all the system investigated had the similar range of frequency factor, but the dependency of the frequency on U_{TP} was not same tendency. In Miller's system, hole diameter of distributor is about 3.1 mm (1 mm in our system) and column diameter is 0.229 m, which is sufficient size to remove wall effect. Therefore at low gas flow rate, coalescence frequency in Miller's system was to expected to be higher than in our system.

CONCLUSIONS

Marrucci model could be applicable to predict the coalescence time of one pair bubble in the dilute solution of electrolytes. The effect of bubble forming frequency on bubble coalescence frequency was investigated. Transition concentration decreased with increase of bubble forming frequency. This tendency was same as the results in low molecular alcohol solution [9].

For a bubble column study, the gas holdup increased with an increase in the gas velocity and electrolyte concentration, caused by the retention of finely dispersed bubbles. The bubble size distribution was narrow for a small gas feed rate or for electrolyte solution. The inhibition effect of bubble coalescence of the K_2SO_4 was slightly higher than that of the KCl at a same ionic strength. In this work, transition concentration was 0.36 kmol/m^3, which is larger than the value predicted in pair bubble study.

NOMENCLATURE

A : Hamaker constant of molecular interactions [J]
c : concentration of solute in film [mol/m^3]
C : $\left(=\frac{2c}{R_G T_e}\left(\frac{d\sigma}{dc}\right)^2\right)$
C_1, C_2 : constants, Eq. (8)
c_i : concentration of ions, i [mol/m^3]
C_o : a constant depending on the geometry of nozzles, the gas flow rate and physical properties of the liquid [$m/s^{1/2}$]
c_t : transition concentration [mol/m^3]
D : diffusion coefficient [m^2/s]
d_B : bubble diameter or equivalent bubble diameter [m]
f : a function of I_{cnt}, h_o and h_f proposed by Marrucci [5]
f_a : activity coefficient
f_c : bubble coalescence frequency [s^{-1}]
f_r : bubble forming frequency [s^{-1}]
h : film thickness [m]
h_f : final film thickness [m]
h_o : initial film thickness [m]
I : ionic strength $\left(=\frac{1}{2}\Sigma c_i z_i^2\right)$
I_{cnt} : Marrucci parameter, as defined in Eq. (1)
k_e : $\left(=\left(\frac{12\pi\sigma}{AR}\right)^{1/3}\right)$
L_i : vertical bubble length [m]
L_m : diameter for which the cumulative distribution curve have a value of 0.5 [m]
N_{BM} : mean bubble concentration [m^{-3}]
N_{Bo} : initial bubble concentration [m^{-3}]
N_p : point bubble frequency [s^{-1}]
$P(L_i)$: probability of a bubble of size L_i existing in a sample of bubbles
ΔP : internal pressure in the film [N/m^2]
R : radius of bubble [m]
R_G : gas constant [J/k·mol]
t_{CO} : elapsed time from bubble contact to coalescence [s]
T_e : temperature [K]
U_G : superficial gas velocity [m/s]
U_{TP} : two phase velocity $[=4(Q_G+Q_L)/\pi d_{BC}^2]$[m/s]
V_{TP} : two phase volume [m^3]
X_D : depth of the diffusion film [m]

z_i : number of charges of ions, i

Greek Letters

α, β : size distribution parameter
ϵ : void fraction
θ : two phase holdup time [$=4V_{TP}/\pi d_{BC}^2 U_{TP}$] [S]
μ : viscosity [Pa·s]
ρ : density [kg/m^3]
σ : surface tension [N/m]
σ_m : ratio of the vertical bubble length for which the cumulative distribution curve has the value of 0.841 to the median vertical bubble length
ϕ : activity coefficient function [$=(1 + d \ln f_a / d \ln c)^{-1}$]

Subscripts

G : gas
L : liquid

REFERENCES

1. Keitel, G. and Onken, V.: *Chem. Eng. Commun.*, **17,** 85 (1982).
2. Walter, J.F. and Blanch, H.W.: *Chem. Eng. J.*, **32,** B7 (1986).
3. Drogaris, G. and Weiland, P.: *Chem. Eng. Sci.*, **38**(9), 1501 (1983).
4. Chuang, K.T., Stirling, A.J. and Baker, J.C.: *I & EC. Fundam.*, **23**(1), 109 (1984).
5. Marrucci, G.: *Chem. Eng. Sci.*, **24**(6), 975 (1969).
6. Sagert, N.H. and Quinn, M.J.: *Can. J. Chem. Eng.*, **57,** 29 (1979).
7. Shah, Y.T., Kelkar, S.P., Godbole, S.P. and Deckwer, W.C.: *AIChE J.*, **28**(3), 353 (1982).
8. Andrew, S.P.S.: in International Symposium on Distillation, edited by Rottenburg, D.A., Institution of Chemical Engineering, London (1960).
9. Kim, J.W. and Lee, W.K.: *J. Chem. Eng. Japan,* **20**(5), 448 (1987).
10. Skelland, A.H.P.: "Diffusional Mass Transfer", John Wiley & Sons, Inc., New York, U.S.A. (1974).
11. Walter, J.F.: Ph.D. Dissertation, University of California, Berkeley (1983).
12. Jin, G.T.: Ph.D. Dissertation, Korea Advanced Institute of Science & Technology (1985).
13. Kim, J.W. and Lee, W.K.: *J. Colloid Interface Sci.*, **123**(1), 303 (1988).
14. Lessard, R.R. and Zieminski, S.A.: *Ind. Eng. Chem. Fundam.*, **10**(2), 260 (1971).
15. Oolman, T.O. and Blanch, H.W.: *Chem. Eng. Commun.*, **43,** 237 (1986).
16. Choi, K.H., Kim, J.W. and Lee, W.K.: *Korean J. Chem. Eng.*, **3**(2), 127 (1986).
17. Himmelblau, D.M.: "Process Analysis by Statistical Methods", John Wiley, New York, (1970).
18. Zieminski, S.A. and Whittemore, R.C.: *Chem. Eng. Sci.*, **26,** 509 (1971).
19. Marrucci, G. and Nicodemo, L.: *Chem. Eng. Sci.*, **22,** 1257 (1967).
20. Akita, K. and Yoshida: *Ind. Eng. Chem. Process. Des. Develop.*, **13**(1), 84 (1974).
21. Hikita, H., Asai, S., Tanigawa, K., Segawa, K. and Kitao, M.: *Chem. Eng. J.*, **20,** 59 (1980).
22. Kelkar, B.G., Phulgaonkar, S.R. and Shah, Y.T.: *Chem. Eng. J.*, **27,** 125 (1983).
23. Freedman, W. and Davidson, J.F.: *Trans. Inst. Chem. Eng.*, **47,** T251 (1969).
24. Kim, S.D., Baker, C.G.T. and Bergougnou, M.A.: *Can. J. Chem. Eng.*, **50,** 695 (1972).
25. Hikita, H. and Kikukawa, H.: *Chem. Eng. J.*, **8,** 19 (1974).
26. Bach, H.F. and Philhofer, T.: *Germ. Chem. Eng.*, **1,** 270 (1978).
27. Mersmann, A.: *Germ. Chem. Eng.*, **1,** 1 (1978).
28. Miller, D.N.: *AIChE J.*, **29**(2), 312 (1983).
29. Davidson, L. and Amick, Jr.A.H.: *AIChE J.*, **2,** 337 (1956).
30. Leibson, I., Hocomb, E.G., Cacoso, A.G. and Jacmic, J.J.: *AIChE J.*, **2**(3), 296 (1956).
31. Bhavaraju, S.M., Russell, T.W.F. and Blanch, H.W.: *AIChE J.*, **44,** 454 (1978).